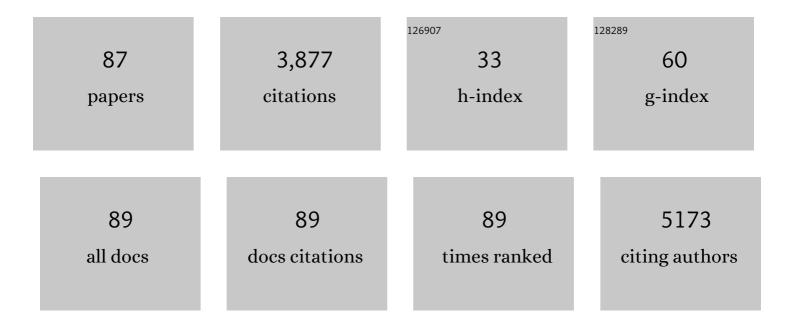
## **ChulHee Kang**

List of Publications by Year in descending order

Source: https://exaly.com/author-pdf/2727004/publications.pdf Version: 2024-02-01



#	Article	IF	CITATIONS
1	A soluble α-synuclein construct forms a dynamic tetramer. Proceedings of the National Academy of Sciences of the United States of America, 2011, 108, 17797-17802.	7.1	408
2	Crystal structure of calsequestrin from rabbit skeletal muscle sarcoplasmic reticulum. Nature Structural Biology, 1998, 5, 476-483.	9.7	212
3	Functional reclassification of the putative cinnamyl alcohol dehydrogenase multigene family in Arabidopsis. Proceedings of the National Academy of Sciences of the United States of America, 2004, 101, 1455-1460.	7.1	210
4	Structure of limonene synthase, a simple model for terpenoid cyclase catalysis. Proceedings of the National Academy of Sciences of the United States of America, 2007, 104, 5360-5365.	7.1	209
5	A Genomewide Analysis of the Cinnamyl Alcohol Dehydrogenase Family in Sorghum [ <i>Sorghum bicolor</i> (L.) Moench] Identifies <i>SbCAD2</i> as the <i>Brown midrib6</i> Gene. Genetics, 2009, 181, 783-795.	2.9	161
6	<i>Brown midrib2</i> ( <i>Bmr2</i> ) encodes the major 4 oumarate:coenzymeâ€fA ligase involved in lignin biosynthesis in sorghum ( <i>Sorghum bicolor</i> (L.) Moench). Plant Journal, 2012, 70, 818-830.	5.7	145
7	Comparing Skeletal and Cardiac Calsequestrin Structures and Their Calcium Binding. Journal of Biological Chemistry, 2004, 279, 18026-18033.	3.4	128
8	Phenylalanine Biosynthesis in Arabidopsis thaliana. Journal of Biological Chemistry, 2007, 282, 30827-30835.	3.4	110
9	Polymerization of Calsequestrin. Journal of Biological Chemistry, 2003, 278, 16176-16182.	3.4	109
10	Biochemical and Structural Analysis of Substrate Specificity of a Phenylalanine Ammonia-Lyase. Plant Physiology, 2018, 176, 1452-1468.	4.8	99
11	Crystal structures and catalytic mechanism of the Arabidopsis cinnamyl alcohol dehydrogenases AtCAD5 and AtCAD4. Organic and Biomolecular Chemistry, 2006, 4, 1687.	2.8	97
12	Modulation of the Redox Potential of the [Fe(SCys)4] Site in Rubredoxin by the Orientation of a Peptide Dipoleâ€. Biochemistry, 1999, 38, 14803-14809.	2.5	91
13	Elucidation of the Structure and Reaction Mechanism of Sorghum Hydroxycinnamoyltransferase and Its Structural Relationship to Other Coenzyme A-Dependent Transferases and Synthases  Â. Plant Physiology, 2013, 162, 640-651.	4.8	82
14	Structure–Function Relationships in Ca2+ Cycling Proteins. Journal of Molecular and Cellular Cardiology, 2002, 34, 897-918.	1.9	75
15	Characterization of Human Cardiac Calsequestrin and its Deleterious Mutants. Journal of Molecular Biology, 2007, 373, 1047-1057.	4.2	69
16	Characterization of Chlorophenol 4-Monooxygenase (TftD) and NADH:FAD Oxidoreductase (TftC) of Burkholderia cepacia AC1100. Journal of Biological Chemistry, 2010, 285, 2014-2027.	3.4	66
17	A common core for binding single-stranded DNA: structural comparison of the single-stranded DNA-binding proteins (SSB) fromE. coliand human mitochondria. FEBS Letters, 1997, 411, 313-316.	2.8	64
18	Mechanistic and Structural Studies of Apoform, Binary, and Ternary Complexes of the Arabidopsis Alkenal Double Bond Reductase At5g16970. Journal of Biological Chemistry, 2006, 281, 40076-40088.	3.4	60

#	Article	IF	CITATIONS
19	Characterization of <i>Solanum tuberosum</i> Multicystatin and Its Structural comparison with Other Cystatins. Plant Cell, 2009, 21, 861-875.	6.6	56
20	High-capacity Ca2+ Binding of Human Skeletal Calsequestrin. Journal of Biological Chemistry, 2012, 287, 11592-11601.	3.4	56
21	Calsequestrin depolymerizes when calcium is depleted in the sarcoplasmic reticulum of working muscle. Proceedings of the National Academy of Sciences of the United States of America, 2017, 114, E638-E647.	7.1	55
22	Crystal structures of vegetative soybean lipoxygenase VLX-B and VLX-D, and comparisons with seed isoforms LOX-1 and LOX-3. Proteins: Structure, Function and Bioinformatics, 2006, 65, 1008-1020.	2.6	53
23	Crystal Structures of Apo-form and Binary/Ternary Complexes of Podophyllum Secoisolariciresinol Dehydrogenase, an Enzyme Involved in Formation of Health-protecting and Plant Defense Lignans. Journal of Biological Chemistry, 2005, 280, 12917-12926.	3.4	51
24	Interaction between Cardiac Calsequestrin and Drugs with Known Cardiotoxicity. Molecular Pharmacology, 2005, 67, 97-104.	2.3	49
25	Inflammation-induced radioresistance is mediated by ROS-dependent inactivation of protein phosphatase 1 in non-small cell lung cancer cells. Apoptosis: an International Journal on Programmed Cell Death, 2015, 20, 1242-1252.	4.9	48
26	Leucine 41 is a gate for water entry in the reduction of <i>Clostridium pasteurianum</i> rubredoxin. Protein Science, 2001, 10, 613-621.	7.6	46
27	The Structure and Catalytic Mechanism of <i>Sorghum bicolor</i> Caffeoyl-CoA <i>O</i> -Methyltransferase. Plant Physiology, 2016, 172, 78-92.	4.8	46
28	Characterization of Class III Peroxidases from Switchgrass. Plant Physiology, 2017, 173, 417-433.	4.8	43
29	Programmed chloroplast destruction during leaf senescence involves 13-lipoxygenase (13-LOX). Proceedings of the National Academy of Sciences of the United States of America, 2016, 113, 3383-3388.	7.1	40
30	Crystal Structures of NADH:FMN Oxidoreductase (EmoB) at Different Stages of Catalysis. Journal of Biological Chemistry, 2008, 283, 28710-28720.	3.4	39
31	S-Clutathionyl-(chloro)hydroquinone reductases: a novel class of glutathione transferases. Biochemical Journal, 2010, 428, 419-427.	3.7	37
32	Inhibitory effect of traditional oriental medicine-derived monoamine oxidase B inhibitor on radioresistance of non-small cell lung cancer. Scientific Reports, 2016, 6, 21986.	3.3	37
33	Structure and Function of the Cytochrome P450 Monooxygenase Cinnamate 4-hydroxylase from <i>Sorghum bicolor</i> . Plant Physiology, 2020, 183, 957-973.	4.8	36
34	Characterizations of Two Bacterial Persulfide Dioxygenases of the Metallo-β-lactamase Superfamily. Journal of Biological Chemistry, 2015, 290, 18914-18923.	3.4	34
35	Raman Signature of the Four-Stranded Intercalated Cytosine Motif in Crystal and Solution Structures of DNA Deoxycytidylates d(CCCT) and d(C8)â€. Biochemistry, 1996, 35, 5747-5755.	2.5	33
36	Determination of the Structure and Catalytic Mechanism of <i>Sorghum bicolor</i> Caffeic Acid <i>O</i> -Methyltransferase and the Structural Impact of Three <i>brown midrib12</i> Mutations Â. Plant Physiology, 2014, 165, 1440-1456.	4.8	33

#	Article	IF	CITATIONS
37	Secoisolariciresinol dehydrogenase: mode of catalysis and stereospecificity of hydride transfer in Podophyllum peltatum. Organic and Biomolecular Chemistry, 2006, 4, 808.	2.8	32
38	The Enzyme Activity and Substrate Specificity of Two Major Cinnamyl Alcohol Dehydrogenases in Sorghum ( <i>Sorghum bicolor</i> ), SbCAD2 and SbCAD4. Plant Physiology, 2017, 174, 2128-2145.	4.8	32
39	Dissociation of MIFâ€rpS3 Complex and Sequential NFâ€̂PB Activation Is Involved in IRâ€Induced Metastatic Conversion of NSCLC. Journal of Cellular Biochemistry, 2015, 116, 2504-2516.	2.6	31
40	Role of Junctin Protein Interactions in Cellular Dynamics of Calsequestrin Polymer upon Calcium Perturbation. Journal of Biological Chemistry, 2012, 287, 1679-1687.	3.4	30
41	Structural and Biochemical Characterization of Cinnamoyl-CoA Reductases. Plant Physiology, 2017, 173, 1031-1044.	4.8	29
42	Structural and Catalytic Differences between Two FADH2-Dependent Monooxygenases: 2,4,5-TCP 4-Monooxygenase (TftD) from Burkholderia cepacia AC1100 and 2,4,6-TCP 4-Monooxygenase (TcpA) from Cupriavidus necator JMP134. International Journal of Molecular Sciences, 2012, 13, 9769-9784.	4.1	28
43	Substrate channeling in oxylipin biosynthesis through a protein complex in the plastid envelope of <i>Arabidopsis thaliana</i> . Journal of Experimental Botany, 2019, 70, 1483-1495.	4.8	28
44	Characterization of Two Human Skeletal Calsequestrin Mutants Implicated in Malignant Hyperthermia and Vacuolar Aggregate Myopathy. Journal of Biological Chemistry, 2015, 290, 28665-28674.	3.4	27
45	Multicolor nanoprobes based on silica-coated gadolinium oxide nanoparticles with highly reduced toxicity. RSC Advances, 2016, 6, 19758-19762.	3.6	26
46	Structural characterization of 2,6â€dichloroâ€ <i>p</i> â€hydroquinone 1,2â€dioxygenase ( <scp>PcpA</scp> ) from <i><scp>S</scp>phingobium chlorophenolicum</i> , a new type of aromatic ringâ€cleavage enzyme. Molecular Microbiology, 2013, 88, 523-536.	2.5	24
47	Folate polyglutamylation eliminates dependence of activity on enzyme concentration in mitochondrial serine hydroxymethyltransferases from Arabidopsis thaliana. Archives of Biochemistry and Biophysics, 2013, 536, 87-96.	3.0	23
48	Effects of Drugs with Muscle-Related Side Effects and Affinity for Calsequestrin on the Calcium Regulatory Function of Sarcoplasmic Reticulum Microsomes. Molecular Pharmacology, 2005, 68, 1708-1715.	2.3	22
49	ALLENE OXIDE SYNTHASE and HYDROPEROXIDE LYASE, Two Non-Canonical Cytochrome P450s in Arabidopsis thaliana and Their Different Roles in Plant Defense. International Journal of Molecular Sciences, 2019, 20, 3064.	4.1	22
50	Inhibition of hedgehog signalling attenuates <scp>UVB</scp> â€induced skin photoageing. Experimental Dermatology, 2015, 24, 611-617.	2.9	21
51	Phosphorylation of human calsequestrin: implications for calcium regulation. Molecular and Cellular Biochemistry, 2011, 353, 195-204.	3.1	19
52	Glycosylation of Skeletal Calsequestrin. Journal of Biological Chemistry, 2012, 287, 3042-3050.	3.4	18
53	Crystallographic studies of V44 mutants of Clostridium pasteurianum rubredoxin: Effects of side-chain size on reduction potential. Proteins: Structure, Function and Bioinformatics, 2004, 57, 618-625.	2.6	17
54	Quantitative improvement of 16S rDNA DGGE analysis for soil bacterial community using real-time PCR. Journal of Microbiological Methods, 2009, 78, 216-222.	1.6	17

#	Article	IF	CITATIONS
55	Structures of the Inducer-Binding Domain of Pentachlorophenol-Degrading Gene Regulator PcpR from Sphingobium chlorophenolicum. International Journal of Molecular Sciences, 2014, 15, 20736-20752.	4.1	17
56	Molecular parallelism in fast-twitch muscle proteins in echolocating mammals. Science Advances, 2018, 4, eaat9660.	10.3	17
57	The unique hydrogen bonded water in the reduced form of Clostridium pasteurianum rubredoxin and its possible role in electron transfer. Journal of Biological Inorganic Chemistry, 2004, 9, 423-428.	2.6	16
58	Structural and biochemical characterization of EDTA monooxygenase and its physical interaction with a partner flavin reductase. Molecular Microbiology, 2016, 100, 989-1003.	2.5	16
59	Sequence-structure mapping errors in the PDB: OB-fold domains. Protein Science, 2004, 13, 1594-1602.	7.6	15
60	Structural studies of Myceliophthora Thermophila Laccase in the presence of deep eutectic solvents. Enzyme and Microbial Technology, 2021, 150, 109890.	3.2	15
61	Furfural reduction mechanism of a zincâ€dependent alcohol dehydrogenase from <i>Cupriavidus necator</i> JMP134. Molecular Microbiology, 2012, 83, 85-95.	2.5	14
62	Potential role of cardiac calsequestrin in the lethal arrhythmic effects of cocaine. Drug and Alcohol Dependence, 2013, 133, 344-351.	3.2	14
63	Structural Understanding of the Glutathione-dependent Reduction Mechanism of Glutathionyl-Hydroquinone Reductases. Journal of Biological Chemistry, 2012, 287, 35838-35848.	3.4	13
64	Characterization of Post-Translational Modifications to Calsequestrins of Cardiac and Skeletal Muscle. International Journal of Molecular Sciences, 2016, 17, 1539.	4.1	13
65	Potential adverse interaction of human cardiac calsequestrin. European Journal of Pharmacology, 2010, 646, 12-21.	3.5	11
66	Crystal structures of unligated and CN-ligatedGlycera dibranchiata monomer ferric hemoglobin components III and IV. Proteins: Structure, Function and Bioinformatics, 2002, 49, 49-60.	2.6	10
67	Structural destabilization of tropomyosin induced by the cardiomyopathyâ€ŀinked mutation R21H. Protein Science, 2018, 27, 498-508.	7.6	8
68	Molecular Mechanisms of Pharmaceutical Drug Binding into Calsequestrin. International Journal of Molecular Sciences, 2012, 13, 14326-14343.	4.1	7
69	Substrate binding properties of potato tuber ADPâ€glucose pyrophosphorylase as determined by isothermal titration calorimetry. FEBS Letters, 2015, 589, 1444-1449.	2.8	7
70	Structural and Functional Characterization of Dynamic Oligomerization in Burkholderia cenocepacia HMG-CoA Reductase. Biochemistry, 2019, 58, 3960-3970.	2.5	7
71	Crystallization and Structure-Function of Calsequestrin. , 2002, 172, 281-294.		6
72	Functional and structural insight into the flexibility of cytochrome P450 reductases from Sorghum bicolor and its implications for lignin composition. Journal of Biological Chemistry, 2022, 298, 101761.	3.4	6

#	Article	IF	CITATIONS
73	Purification, crystallization and preliminary crystallographic studies of the ligand-binding domain of a plant vacuolar sorting receptor. Acta Crystallographica Section D: Biological Crystallography, 2004, 60, 2028-2030.	2.5	5
74	The role of backbone stability near Ala44 in the high reduction potential class of rubredoxins. Proteins: Structure, Function and Bioinformatics, 2005, 62, 708-714.	2.6	4
75	A Ligandâ€Directed Nitrophenol Carbonate for Transient in situ Bioconjugation and Drug Delivery. ChemMedChem, 2020, 15, 2004-2009.	3.2	3
76	Site-Specific Synthesis of Cysteine-Bridged Glycoproteins via Expressed Protein Glycoligation. Bioconjugate Chemistry, 2020, 31, 2362-2366.	3.6	3
77	The Structural Basis of the Binding of Various Aminopolycarboxylates by the Periplasmic EDTA-Binding Protein EppA from Chelativorans sp. BNC1. International Journal of Molecular Sciences, 2020, 21, 3940.	4.1	3
78	Conformational Rearrangements in the Redox Cycling of NADPH-Cytochrome P450 Reductase from Sorghum bicolor Explored with FRET and Pressure-Perturbation Spectroscopy. Biology, 2022, 11, 510.	2.8	3
79	Characterization of Interactions between CTX-M-15 and Clavulanic Acid, Desfuroylceftiofur, Ceftiofur, Ampicillin, and Nitrocefin. International Journal of Molecular Sciences, 2022, 23, 5229.	4.1	3
80	Vascular Plant Lignification: Biochemical/Structural Biology Considerations of Upstream Aromatic Amino Acid and Monolignol Pathways. , 2010, , 541-604.		2
81	Crystal Structure of Phosphoserine BlaC from Mycobacterium tuberculosis Inactivated by Bis(Benzoyl) Phosphate. International Journal of Molecular Sciences, 2019, 20, 3247.	4.1	1
82	Structural and biochemical characterization of iminodiacetate oxidase from Chelativorans sp. BNC1. Molecular Microbiology, 2019, 112, 1863-1874.	2.5	1
83	Thermodynamic Driving Forces of Redox-Dependent CPR Insertion into Biomimetic Endoplasmic Reticulum Membranes. Journal of Physical Chemistry B, 2022, 126, 1691-1699.	2.6	1
84	Excreted Antibiotics May Be Key to Emergence of Increasingly Efficient Antibiotic Resistance in Food Animal Production. Applied and Environmental Microbiology, 2022, 88, .	3.1	1
85	Argentine Worker Ant (Hymenoptera: Formicidae) Mortality Response to Sodium Salicylate and Sodium Cinnamate. Journal of Entomological Science, 2014, 49, 342-351.	0.3	0
86	Bis(benzoyl) phosphate inactivators of beta-lactamase C from Mtb. Bioorganic and Medicinal Chemistry Letters, 2019, 29, 2116-2118.	2.2	0
87	Extension of the four-stranded intercalated cytosine motif by adenine•adenine base pairing in the crystal structure of d(CCCAAT). journal of hand surgery Asian-Pacific volume, The, 2018, , 275-284.	0.4	0